9th LECTURE
4th April, 1963.

NEUTRINO SPECTRA FROM THE TWO-BODY DECAY OF RELATIVISTIC PARENTS

by C. A. Ramm

The production of neutrino fluxes at a distance d from a limited isotropic source of monoenergetic relativistic parents, of a particular γ, and decay length λ, is considered in terms of the angular divergence ϕ and flight path r. If $\gamma\phi >> 1$ and $\lambda >> r$ the axial neutrino flux per unit area is $n_1 = \frac{r}{\lambda d}$ per parent per unit solid angle, and the differential energy spectrum extends from $2\gamma E'_\nu$ to zero, so that the mean energy is $\gamma E'_\nu$. If d-r is fixed by shielding requirements, then it is well known that the maximum flux density is for an arrangement where $r = d/2$.

For sources of small divergence the axial neutrino flux per parent is $n_2 = \frac{\gamma^2}{\pi\lambda d} \frac{1}{\gamma\phi} \tan^{-1} \frac{r\gamma\phi}{(1+\gamma^2\phi^2)d-r}$ and the mean energy is

$$\gamma E'_\nu \left(2 - \frac{\gamma^2\phi^2(d^2+(d-r)^2+2\gamma^2\phi^2d^2)}{2(1+\gamma^2\phi^2)((d-r)^2+\gamma^2\phi^2d^2)}\right)$$

Thus if $\gamma\phi << 1$ the maximum achievable axial neutrino flux tends to the limit $\frac{\gamma^2}{\pi\lambda(d-r)}$, with the mean energy $2\gamma E'_\nu$.

The relation between neutrino fluxes from pencil beams and slightly divergent beams of parents is discussed, and the matching between the arrangement of the neutrino detectors and the degree of parent focusing is examined.

Finally the relationships developed in the paper are used to examine the neutrino fluxes which are achievable in principle by pencil focusing of the known parent spectra from the PS.

1. Introduction

The possibility of detection of high energy neutrino interactions provides a timely means to increase knowledge by experiment in an ever widening field of speculative ideas.

These problems are some of the most challenging high energy physics around the large accelerators and the present experiments can but be the forbears of increasingly refined studies. New detectors, new means of producing intense high energy neutrino fluxes and new experiments will be sought to make accessible production thresholds at higher energies and smaller interaction cross-sections, and for the pursuit of such postulates as the intermediate boson.

The aim of this note is to investigate the limitations of the production of neutrino spectra from two-body decay of relativistic parents, and thus to collect data which might be of use in the development of still better neutrino facilities and experimental layouts.

1.1 Kinematics

From the Lorentz transformation the total energy E, momentum p and direction θ in the laboratory system (LS) and centre of mass system (CS) of a particle are related by:

$$E = \gamma(E' + \beta p'\cos\theta') \quad (1)$$

$$p\cos\theta = \gamma(p'\cos\theta' + \beta E') \quad (2)$$

$$p\sin\theta = p'\sin\theta' \quad (3)$$

Primes refer to CS, the system of units has $c = 1$, and $\gamma = (1-\beta^2)^{-\frac{1}{2}}$ is the ratio between the total energy in LS and CS.

Since $p'/E' = \beta'$ it follows that

$$\gamma \tan\theta = \frac{\sin\theta'}{\cos\theta' + \beta/\beta'} \tag{4}$$

$$\frac{dw'}{dw} = \frac{d\theta'}{d\theta}\,\frac{\sin\theta'}{\sin\theta} = \frac{\left[(\cos\theta' + \beta/\beta')^2 + (1-\beta)^2\sin^2\theta'\right]^{3/2}}{(1-\beta)^2\,(1+(\beta\cos\theta')\,/\,\beta')} \tag{5}$$

$$= \frac{\left[\gamma^2(\cos\theta'+\beta/\beta')^2 + \sin^2\theta'\right]^{3/2}}{\gamma(1+(\beta\cos\theta')\,/\,\beta')} \tag{6}$$

For many previous experimental situations convenient relations have been developed from these bases, a recent review by Dedrick[1] gives numerous references. Relations which are of particular convenience in the study of neutrino fluxes will now be derived.

1.2 Angular Distribution of Neutrinos from Relativistic Parents.

If the neutrino parent decays isotropically in CS, then the fraction α of the neutrino production contained in a cone of semi-angle θ' is

$$\alpha = (1-\cos\theta')\,/\,2 \tag{7}$$

For the relativistic case ($\beta=\beta'=1$) this transforms to LS by (4) as

$$\alpha = \gamma^2\tan^2\theta\,/\,(1+\gamma^2\tan^2\theta) \tag{8}$$

The relations (4), (7) and (8) are represented in fig. 1. Clearly the neutrino production in the forward hemisphere in CS transforms to the cone of semi-angle $\tan^{-1} 1/\gamma$ in LS. By differentiation of (8),

$$\frac{d\alpha}{d\theta} = \frac{2\gamma^2 \tan\theta(1+\tan^2\theta)}{(1+\gamma^2\tan^2\theta)^2} \qquad (9)$$

Either directly by the relation $\frac{dw'}{dw} = \frac{2}{\sin\theta}\ \frac{d\alpha}{d\theta}$, or by simplification of (6) for $\beta = 1$,

$$\frac{dw'}{dw} = \frac{4\gamma^2(1+\tan^2\theta)^{3/2}}{(1+\gamma^2\tan^2\theta)^2} \qquad (10)$$

For $\beta = \beta' = 1$ the dependence of the angular distribution on the parent γ alone is at once evident in these relations. From (4), for small angles $2\gamma\theta = \theta'$, which gives a forward kinematic concentration of the neutrino flux in LS of $4\gamma^2$, which is equally evident in (10).

1.3 Neutrino Energy.

If the parent particle of total energy E_p decays into two products, then for each (1), (2) and (3) hold, $p_1' = p_2'$, and $\cos\theta_1' = -\cos\theta_2'$, from conservation of momentum. For a neutrino with zero rest mass $p_\nu = E_\nu$, so that

$$E_\nu = \gamma E_\nu' (1+\beta\cos\theta') \qquad (11)$$

Transforming to LS, and for a relativistic parent ($\beta = 1$),

$$E_\nu = 2\gamma E_\nu'/(1+\gamma^2\tan^2\theta) \qquad (12)$$

Thus the spectrum of neutrino energy from a relativistic parent extends from $2\gamma E_\nu'$ to zero, and from the conservation of energy the spectrum of the companion particle extends from E_p to $E_p - 2\gamma E_\nu'$. This result is shown in fig. 2, together with the spectra of parents for various β.

1.4 Differential Spectrum.

From (8) and (12) the fraction of neutrinos in the energy interval from $2\gamma E'_\nu$ to E_ν is $\alpha = 1-E/2\gamma E'_\nu$

from which $$d\alpha = - dE/2\gamma E'_\nu \qquad (13)$$

Thus the differential energy spectrum of neutrinos from relativistic parents decaying isotropically in CS, is constant. This constancy of the differential energy spectrum of the products from the two-body isotropic decay of a parent is well known, and holds generally, irrespective of the masses of the products, or velocity of the parents.[2)]

The mean energy $\bar{E}_\nu$ of the neutrinos in LS, in the cone of semi-angle θ is $(2\gamma E'_\nu+E_\nu)/2$, which gives from (12) that

$$\bar{E}_\nu = \gamma E'_\nu(2+\gamma^2\tan^2\theta)/(1+\gamma^2\tan^2\theta) \qquad (14)$$

Evidently, for $\theta = \tan^{-1} 1/\gamma$ then $\bar{E}_\nu = 3\gamma E'_\nu/2$.

2. Neutrino Flux from an Isotropic Source of Parents.

Consider an isotropic source of parents (fig. 3) of decay length λ, which have free flight up to an absorber at radius r. From symmetry, and the divergence theorem, the flux of neutrinos per unit surface of spherical shell of radius d, per parent per steradian, is

$$n = a(1 - e^{-\frac{r}{\lambda}})/d^2 \qquad (15)$$

where a is the multiplicity of neutrinos per parent decay, which we shall assume in all the following to be unity. If $\lambda >> r$, then the flux is

$$n_1 = \frac{r}{\lambda d^2} \qquad (16)$$

If the neutrinos are produced by two-body decay from relativistic parents, then from (14) the mean neutrino energy is

$$\bar{E}_\nu = \gamma E'_\nu \qquad (17)$$

3. Neutrino Flux from an Isotropic Parent Cone.

Clearly not all parent decays contribute significantly to the detector in fig. 3. The neutrino flux contributed per parent per steradian in the cone of semi-angle ϕ is,

$$n = \frac{1}{2\lambda}\int_o^r\int_o^{\phi} \frac{e^{-\frac{r}{\lambda}}\sin\phi(d-r\cos\phi)}{(d^2+r^2-2rd\cos\phi)^{3/2}}\left(\frac{dw'}{dw}\right)_\theta d\phi\, dr \qquad (18)$$

where r and d are shown in fig. 4, and $\left(\frac{dw'}{dw}\right)_\theta$ is the transformation of solid angle from CS to LS appropriate to each disintegration. For very slow parents $\left(\frac{dw'}{dw}\right) = 1$ and if $\lambda >> r$ then for $\phi = \pi$, (18) integrates to give directly $n = \frac{r}{\lambda d^2}$ as in (16).

3.1 Relativistic Parents.

The relativistic case is more important. Then $\left(\frac{dw'}{dw}\right)$ is given by (10), which for the conditions of fig. 4 may be written

$$\frac{dw'}{dw} = \frac{4\gamma^2\left(1-\frac{2r}{d}\cos\phi + \frac{r^2}{d^2}\right)^{3/2}\left(\cos\phi - \frac{r}{d}\right)}{\left(\cos^2\phi(1-\gamma^2) - \frac{2r}{d}\cos\phi + \frac{r^2}{d^2} + \gamma^2\right)^2} \qquad (19)$$

$$n = \frac{2\gamma^2}{\lambda}\int_o^r\int_o^{\phi} \frac{e^{-\frac{r}{\lambda}}\sin\phi(d-r\cos\phi)(d\cos\phi-r)}{(\gamma^2d^2(1-\cos^2\phi) + d\cos\phi(d\cos\phi-2r) + r^2)^2}\, d\phi\, dr \qquad (20)$$

For many practical situations ϕ is small, so that $\cos\phi = 1$ and $\cos^2\phi = 1-\phi^2$, and for relativistic parents $\gamma^2 >> 1$, so that approximately,

$$n = \frac{2\gamma^2}{\lambda}\int_o^r\int_o^{\phi} \frac{e^{-\frac{r}{\lambda}\phi(d-r)^2)^2}}{(\gamma^2\phi^2d^2 + (d-r)^2)^2}\, d\phi\, dr \qquad (21)$$

which for $\lambda >> r$ evaluates to

$$n = \frac{\gamma\phi}{\lambda d}\left(\tan^{-1}\frac{1}{\gamma\phi} - \tan^{-1}\frac{d-r}{\gamma\phi d}\right) \qquad (22)$$

or $$n_2' = \frac{\gamma\phi}{\lambda d}\tan^{-1}\frac{r\gamma\phi}{(1+\gamma^2\phi^2)d-r} \qquad (23)$$

which is shown in fig. 5.
For $\gamma\phi = 1$ in (23) $n_2 = \frac{1}{\lambda d}\left(\cdot 785 - \tan^{-1}\frac{d-r}{d}\right)$, from which for $d/2 < r < d$ we see that $0\cdot928 > \frac{n_2}{n_1} > 0\cdot785$. Since n_1 is the maximum possible neutrino flux from an isotropic source of parents, it is evident that only a small fraction of the neutrino flux is contributed from parents outside the cone of semi-angle γ^{-1}. In fact with an error of 21·5 % when $r = d$ and less than 8 % when $r = d/2$ we may write the contribution from this cone as simply n_1.

Evidently the axial flux in the detector plane, per parent contained in the cone of semi-angle ϕ, may be written directly from (22) and (23) as

$$n_2 = \frac{\gamma^2}{\pi\lambda d}\cdot\frac{1}{\gamma\phi}\left(\tan^{-1}\frac{1}{\gamma\phi} - \tan^{-1}\frac{d-r}{\gamma\phi d}\right) \qquad (24)$$

or $$n_2 = \frac{\gamma^2}{\pi\lambda d}\frac{1}{\gamma\phi}\tan^{-1}\frac{r\gamma\phi}{(1+\gamma^2\phi^2)d-r} \qquad (24')$$

which is shown in fig. 6.

3.2 Average Neutrino Energy at the Detector.

The average neutrino energy at the detector is

$$\bar{E}_\nu = \frac{1}{n}\int E_\nu(\phi,r)\frac{dn}{dr}\,dr$$

which, from (18) and (12) may be written

$$\bar{E}_\nu = \frac{1}{2\lambda n} \int_0^r \int_0^{\phi} \frac{e^{-\frac{r}{\lambda}} \sin\phi(d - r\cos\phi)}{(d^2+r^2-2rd\cos\phi)^{3/2}} \left(\frac{dw'}{dw}\right)_\theta \frac{2\gamma E'_\nu}{1+\gamma^2\tan^2\theta} \, d\phi \, dr \quad (25)$$

By analogy with (21), and with the same approximation this reduces to

$$\bar{E}_\nu = \frac{4\gamma^3 E'_\nu}{\lambda n} \int_0^r \int_0^{\phi} \frac{e^{-\frac{\lambda}{r}} \phi (d-r)^4}{(\gamma^2\phi^2 d^2 + (d-r)^2)^3} \, d\phi \, dr \quad (26)$$

and with the assumption $\lambda >> r$ this integrates directly to

$$\bar{E}_\nu = \gamma E'_\nu \left(\frac{3}{2} + \frac{\gamma\phi}{2} \left(\tan^{-1} \frac{1}{\gamma\phi} - \tan^{-1} \frac{d-r}{\gamma\phi d} \right) - \frac{r\,(d - r - \gamma^2\phi^2 d)}{(1+\gamma^2\phi^2)((d-r)^2 + \gamma^2\phi^2 d^2)} \right) \quad (27)$$

For those cases in which it is possible to approximate $\tan^{-1} \frac{r\gamma\phi}{(1+\gamma^2\phi^2)d-r}$ by its tangent, and by rearranging,

$$\bar{E}_\nu = \gamma E'_\nu \left(2 - \frac{\gamma^2\phi^2(d^2+(d-r)^2 + 2\gamma^2\phi^2 d^2)}{2(1+\gamma^2\phi^2)((d-r)^2 + \gamma^2\phi^2 d^2} \right) \quad (28)$$

This relation which contains some of the results already derived is shown in fig. 7. In the limit for $\gamma^2\phi^2 >> 1$ then (28) reverts to $E'_\nu = \gamma E'_\nu$ as for (17), and for $\gamma^2\phi^2 << 1$ it reverts to $\bar{E}_\nu = 2\gamma E'_\nu$, i.e. the maximum neutrino energy of (11). For $r = 0$, $E_\nu = \gamma E'_\nu \, (2+\gamma^2\phi^2)/(1+\gamma^2\phi^2)$ which is consistent with (14) for ϕ small. It is useful to note that for $\gamma\phi = 1$ and $r = d$, $\bar{E}_\nu = 1{\cdot}25 \, \gamma E'_\nu$ and for $r = d/2$, $\bar{E}_\nu = 1{\cdot}35 \, \gamma E'_\nu$.

4.1 Neutrino Flux from a Pencil of Relativistic Parents.

Consider the neutrino distribution, in the detector plane, from relativistic parents in a pencil beam originating from a source at distance d (fig. 8).* From (8) the number of

*Figs. 3, 4, 8, 9 and 11 are on the same page.

neutrinos $n(y)dx$ within a radius y of the point of intersection of the pencil with the detector plane, and which originated in the element dx at x, per parent, is $\alpha\, dx$. The total number of neutrinos within the same circle, originating from the whole pencil is,

$$n(y) = \frac{1}{\lambda}\int_0^x \frac{e^{-\frac{x}{\lambda}}\gamma^2 y^2}{(d-x)^2+\gamma^2 y^2}\, dx$$

For $\lambda >> x$ this integrates to

$$n(y) = \frac{\gamma y}{\lambda}\left[\tan^{-1}\frac{d}{\gamma y} - \tan^{-1}\frac{d-x}{\gamma y}\right] \qquad (29)$$

$$= \frac{\gamma y}{\lambda}\tan^{-1}\frac{x\gamma y}{\gamma^2 y^2+d(d-x)} \qquad (29')$$

which is the same relation as shown in fig. 5 with the substitution $\gamma\phi = \frac{\gamma y}{d}$ and $x = r$.

The mean neutrino flux per unit area within the radius y is

$$n_3 = \frac{\gamma^2}{\pi\lambda d}\,\frac{d}{\gamma y}\cdot A \qquad (30)$$

where A is the angle of (29) and (29') and whose geometrical significance is shown in fig. 9. It is the angle subtended by the parent decay path at a point in the detector plane distant γy from the pencil axis. It is observed that (30) is the same relation as shown in fig. 6 with the same substitutions as for (29).

4.2 Mean Energy of the Neutrino Flux from a Pencil of Relativistic Parents.

The mean energy of the neutrinos within the circle of radius y is

$$\bar{E}_\nu = \frac{1}{n}\int E_\nu(x)\frac{dn}{dx}\, dx$$

From the preceding section, and (14) this becomes

$$\bar{E}_\nu = \frac{\gamma E'_\nu}{n} \int_0^x \frac{\gamma^2 y^2 (2(d-x)^2 + \gamma^2 y^2)}{((d-x)^2 + \gamma^2 y^2)^2} \, dx \qquad (31)$$

On integrating, substituting n from (31), and rearranging,

$$\bar{E}_\nu = \gamma E'_\nu \left(2 - \frac{\gamma^2 y^2 (d^2 + (d-x)^2 + 2\gamma^2 y^2)}{2(d^2+\gamma^2 y^2)((d-x)^2+\gamma^2 y^2)} \right) \qquad (32)$$

which is the same as the relation shown in fig. 7, with the same substitutions as for (29).

4.3 Off-axial Distribution of the Neutrino Flux from Parent Pencil.

The mean neutrino flux at the detector plane, within a radius y from the axis of a pencil beam is given by (29), from which

$$\frac{dn}{dy} = \frac{\gamma}{\lambda} \tan^{-1} \frac{x\gamma y}{\gamma^2 y^2 + d(d-x)} + \frac{\gamma^2 xy}{\lambda} \frac{(d^2 - dx - \gamma^2 y^2)}{(d^2+\gamma^2 y^2)((d-x)^2+\gamma^2 y^2)}$$

so that the neutrino flux per unit area at radius y is

$$N(y) = \frac{1}{2\pi y} \frac{dn}{dy} = \frac{\gamma}{2\pi\lambda y} \left[\tan^{-1} \frac{x\gamma y}{\gamma^2 y^2 + d(d-x)} + \frac{x\gamma y (d^2 - dx - \gamma^2 y^2)}{(d^2+\gamma^2 y^2)((d-x)^2+\gamma^2 y^2)} \right] \qquad (33)$$

This relation is shown in fig. 10.

In a practical experimental layout, if $x \ll d$ it may be sufficient to replace the angle in (33) by its tangent, in which case,

$$N(y) \sim \frac{\gamma^2 x}{2\pi\lambda} \frac{(2d^2(d-x)^2 + \gamma^2 y^2 (d^2 + (d-x)^2))}{(d^2+\gamma^2 y^2)(d(d-x)+\gamma^2 y^2)((d-x)^2+\gamma^2 y^2)} \qquad (34)$$

For the particular case of $x = 0$ the neutrino flux

per unit annulus at y, is

$$N = \frac{dn}{dy} = \frac{2\gamma^2 y/d}{\left(1+\frac{\gamma^2 y^2}{d^2}\right)^2} \cdot \frac{x}{\lambda d} \text{ , which is consistent}$$

with (9) for $\tan^2\theta$ negligible compared with unity.
$\left(\frac{y}{d} = \theta \text{ and } \frac{dn}{dy} = \frac{x}{\lambda d}\frac{d\alpha}{d\theta}\right)$.

4.4 Radial Distribution of Neutrino Flux from Extensive Parent Beam.

For simplicity consider a parent beam of such an intensity that there is one trajectory per unit area in its projection to the detector plane, i.e. with an intensity of d^2 parents per steradian. In principle the neutrino flux per unit area in the detector plane may be found directly from the integration, over the appropriate space, of the product of $N(y)$ given by (33) with the parent intensity.

Suppose for example a conical beam of parents of uniform intensity of one parent per steradian, which interacts in the circle of radius r in the detector plane. The intensity at a point distance a from the axis contributed by those parents in the element dy is, for $r > a$,

$$I = \frac{2}{d^2}\left[\int_{y=r-a}^{y=r+a} N(y) \cos^{-1}\frac{y^2+a^2-r^2}{2ay}\, dy + \int_{y=o}^{y=(r-a)} N(y)\, dy\right] \qquad (35)$$

For the case $r < a$

$$I = \frac{2}{d^2}\int_{r-a}^{r+a} N(y) \cos^{-1}\frac{y^2+a^2-r^2}{2ay}\, dy \qquad (35')$$

These expressions may be evaluated numerically, and with some elaboration they may be amplified to take account of any

parent distribution. With the curves of fig. 10 it is possible, by inspection, to obtain some indication of the relative importance of the flux contribution from various parts of the parent beam.

4.5 Average Energy of the Off-axial Neutrino Flux.

Consider again fig. 8. From (9) the neutrino flux in the annulus dy, at the radius y, originating between x and x+dx per parent is

$$N(x,y)dx = \frac{1}{\lambda}\frac{d\alpha}{d\theta}\frac{d\theta}{dy}\,dx$$

$$= \frac{2\gamma^2}{\lambda}\frac{\tan\theta}{(d-x)(1+\gamma^2\tan^2\theta)^3}\,dx$$

The energy of these neutrinos is

$$E_\nu(x,y) = \frac{2\gamma E'_\nu}{1+\gamma^2\tan^2\theta}$$

The mean energy is thus

$$\bar{E}_\nu(y) = \frac{\frac{4\gamma^3 E'_\nu}{\lambda}\int_0^x \frac{\tan\theta}{(d-x)(1+\gamma^2\tan^2\theta)^3}\,dx}{\int N(x,y)\,dx}$$

Substitute $\tan\theta = \frac{y}{d-x}$, and with $N(y)$ already determined from (34)

$$\bar{E}_\nu(y) = \frac{2\gamma^3 E'_\nu}{\pi\lambda N(y)}\int_0^x \frac{(d-x)^4}{((d-x)^2+\gamma^2y^2)^3}\,dx \qquad (36)$$

$$= \frac{2\gamma^3 E'_\nu}{\pi\lambda N(y)}\left[\frac{(d-x)(5(d-x)^2+3\gamma^2y^2)}{8((d-x)^2+\gamma^2y^2)^2} - \frac{d(5d^2+3\gamma^2y^2}{8(d^2+\gamma^2y^2} + \right.$$

$$\left. + \frac{3}{8\gamma y}\left(\tan^{-1}\frac{d}{\gamma y} - \tan^{-1}\frac{d-x}{\gamma y}\right)\right] \qquad (37)$$

By substituting $N(y)$ from (33) the off-axial energy distribution from the pencil may be evaluated. In order to determine the off-axial energy distribution from a cone a procedure similar to that used in preceding sections may be used to develop the mean energy distribution from the integrals of (35) and (36), which must then be evaluated numerically.

4.6 The Relation between the Neutrino Fluxes from a Pencil and a Small Cone of Parents.

The pairs of relationships (24), (29), and (28), (32) have obvious similarities. In fact we could have deduced one of the pair from the other by simple geometrical considerations.

Suppose a divergent beam of parents of intensity one trajectory per unit area in the detector plane. Consider a parent decaying at A, at the corresponding decay of a pencil parent at A' (fig. 11). If ϕ is small so that θ and θ' are sensibly equal, the flux contributed per unit area at the axis in the detector plane, per parent at A, is $\frac{1}{2\pi y}$ of the flux in the annulus of unit width at y, produced at A' by the pencil parent. For the conditions chosen there are just $2\pi y$ parent trajectories per unit annulus at y.

Thus for all possible contributions of the parent cone up to ϕ the neutrino flux per unit area in the detector plane, at the axis, is equal in intensity and energy distribution to the total neutrino flux, within the circle of radius y, produced by a single axial parent.

However the parent intensity per steradian under the conditions chosen is $\pi y^2 / \pi \phi^2 = d^2$. Thus the total neutrino flux from a single axial parent in the circle intercepted by the cone semi-angle ϕ is d^2 times the flux per unit area at the axis, if the cone is filled with parents of unit density per steradian, has the same differential energy spectrum. In fact this is precisely the relationship between the formulae already derived.

5.1 Choice of Optimum Length of Parent Cone. ($\lambda >> r$)

In an experimental arrangement of a neutrino beam the shielding thickness t may be determined by considerations independent of the parents associated with a useful neutrino flux. Rewriting (25) in terms of t

$$n_2' = \frac{\gamma^2}{\pi\lambda\gamma\phi} \frac{1}{t+r} \tan^{-1} \frac{r\gamma\phi}{(1+\gamma^2\phi^2)t+r\gamma^2\phi^2} \tag{38}$$

The axial neutrino flux per parent in the cone of semi-angle ϕ is shown in fig. 12. Both the rapid increase of the axial flux with parent focusing, and the relative insensitivity for $\frac{r}{t} > 1$ are at once evident. To choose r for a particular $\gamma\phi$, so that the flux per unit area at the axis is a maximum, set $\frac{dn'}{dr} = 0$, whence

$$\frac{\gamma\phi(\gamma^2\phi^2+1)(1+\frac{r}{t})}{(\gamma^2\phi^2+1) + \frac{r}{t}\gamma^2\phi^2)^2 + \frac{r^2}{t^2}\gamma^2\phi^2} = \tan^{-1}\frac{\frac{r}{t}\gamma\phi}{\gamma^2\phi^2(1+\frac{r}{t})+1} \tag{39}$$

For cases in which the angle on the right may be approximated by its tangent the condition reduces to

$$\left(\frac{r}{t}\right)^3 + \left(\frac{r}{t}\right)^2 - \frac{r}{t} = (1+\gamma^2\phi^2)/\gamma^2\phi^2 \tag{40}$$

If $\gamma\phi >> 1$, then $r = t$ satisfies the relation, which is the well known optimisation of n_1 in (16). Optimum values of $\frac{r}{t}$ for various values of $\gamma\phi$ are shown in fig. 13. For $\lambda >> r$ these values are of little practical importance because of the uncritical nature of the optimisation already noted, but if $\lambda \not< t$ the situation may be changed significantly, and of course (39) no longer obtains.

For $\gamma\phi << 1$ then

$$n_2' = \frac{\gamma^2}{\pi\lambda t} \frac{r}{t+r} \tag{41}$$

$$\sim \frac{\gamma^2}{\pi\lambda t} \quad \text{for} \quad r >> t \neq 0, \tag{41'}$$

and thus under these conditions the maximum achievable neutrino flux per parent varies inversely as the shielding thickness.

5.2 Optimisation of Parent Pencil.

By the analogy of 4.5, $\gamma\phi$ can be replaced by $\gamma y/d$, and the optimisation and figures then refer to the average neutrino flux contained in the circle of radius y in the detector plane. The result of (41') might have to be anticipated directly, since the angle subtended by a semi-infinite line source at a point near the axis varies inversely as its distance from the nearest point of the source.

6. On the Realization of Maximum Neutrino Fluxes.

From preceding studies it is clear that the maximum axial flux in the detector plane, per parent, is produced by both pencil focusing of the parents and using the minimum possible shielding thickness. From (38) and fig. 12, for $\lambda >> r$ it was seen that very little increase in axial flux is obtained by making the decay path longer than the shielding thickness. The maximum achievable axial flux is almost linear with the reciprocal of the shielding thickness, which has been the basis of proposals for the use of high density absorbers, such as lead or even uranium. These possibilities have been examined by Fowler and Perkins[3] in connection with possible neutrino experiments at Nimrod. In practice the shielding has to be designed to attenuate all background fluxes to a tolerable level. In the Brookhaven and proposed CERN experiments the shielding thickness is determined by muons, whose parents are of such rarity as to make no useful contribution to the neutrino flux. At lower energy accelerators the neutrons may impose the limiting shielding parameters. With any focusing device producing directly a parent pencil from a target it is difficult to imagine a means of separating and absorbing the undesirable high energy parents from the lower energy spectrum, and hence the shielding may be excessively thick.

A simple principle which is being studied and which might be useful in a future experimental arrangement is shown in fig. 14. By means of a reflecting device, useful parents from a strongly divergent source could be returned to form a beam convergent at the detector. Clearly the convergent parent beam has all the properties of a pencil beam for production of the neutrino flux, and it is also evident that the shielding can be redistributed, and that part immediately in front of the detector reduced to the minimum appropriate to the background produced by the highest energy useful parents, or the neutron production from their interaction in the shielding. Unfortunately it is also evident that the technological problems of achieving such a device are profound.

6.1 Possible Neutrino Fluxes from the PS.

Finally it is interesting to use the relations derived in the preceding section to estimate the neutrino spectra achievable under various conditions from the PS. As basic data the experimental spectra from Brookhaven[4] and CERN[5] have been integrated to give the available fluxes of pions and kaons, assuming an average of one interaction of 25 GeV primary protons in a target. The results are shown as differential neutrino spectra in fig. 15 and as integral spectra in fig. 16. For the pencil beams it has been assumed that the focusing device was free from absorption, and for all calculations it has been assumed that $\lambda >> r$. For the calculations of the neutrino flux from a free target, the parent distribution has been assumed uniform up to $\tan^{-1}\gamma^{-1}$, but to allow some compensation for the natural forward peaking, $1{\cdot}35\ \gamma E'_\nu$ has been taken as the energy appropriate to the neutrinos, but the intensity has been augmented by a factor of 1·4, the intensity appropriate to $\tan^{-1}2\gamma^{-1}$. (vide 3.2)

In fig. 15 the numbers beside the calculated points indicate the upper limit in the parent spectrum necessary to maintain the neutrino spectrum shown, up to the position of that number. The following data have been estimated for fig. 15, and most also for fig. 16.

Ejected proton beam of 25 GeV on Be target, one interaction per proton, no parent absorption.

Axial neutrinos from natural parent spectrum (r = 25 M d = 50 M)

Curve 1 From pions of either sign.
Curve 2 From positive kaons.
Curve 3 From negative kaons.

Axial neutrino flux from pencil parents

x = 25 M d = 50 M
Curve 4 From pions of either sign.
Curve 5 From positive kaons.
Curve 6 From negative kaons.

x = 10 M d = 50 M
Curve 7 From pions of either sign.
Curve 8 From positive kaons.

x = 5 M d = 50 M
Curve 9 From pions of either sign.
Curve 10 From positive kaons.

The negative kaon curves for x = 10 M and x = 5 M have the same displacements as the positive kaon curves.

Neutrino flux averaged over circle of diameter 1 M from pencil focused parents (x = 25 M d = 50 M).

Curve 11 Pions of either sign.
Curve 12 Positive kaons.
Curve 13 Negative kaons.

For comparison the following curves have also been included:

From computations of S. van der Meer (r = 23·5 M d = 48·25 M)

Curve 14 Axial neutrinos from natural pion spectrum, no absorption.

Neutrino flux with magnetic horn at 300 kA, with absorption.

Curve 15 From focused pions.
Curve 16 From focused positive kaons.
Curve 17 From defocused kaons.

Neutrinos with magnetic horn at zero current, with absorption

Curve 18 From pions.

Pencil focused parents, without absorption

Curve 19 From pions.

Also included are

Curve 20 Neutrinos from pions in the Brookhaven-Columbia-experiment (6)
Curve 21 Neutrinos from kaons in the Brookhaven-Columbia-experiment (6)
Curve 22 Neutrinos from pions in the first CERN experiment.

* * *

ACKNOWLEDGEMENTS

It is a pleasure to acknowledge the constructive criticisms and suggestions of Drs. D. Cundy and K. Schultze who read the first draft of this paper, to thank Dr. S. van der Meer for the data he has provided for figures 15 and 16, and to thank Mrs. V. Donat and D. Métral, Misses S. Dubois and A. Labet and Messrs. A. Dind and A. Duty for their unstinted efforts in variously computing and constructing the curves and organizing the preparation of the paper.

REFERENCES

1. K. G. Dedrick, R.M.P. 31, 3 1962.
2. e.g. B. Rossi, High Energy Particles, Prentice Hall - New York, 191, 1952.
3. P. H. Fowler and D. H. Perkins. Private communication.
4. W. F. Baker et al, Phys. Rev. Letters 7, 101, 1961.
5. A. N. Diddens et al, Data on Negative Particle Spectra CERN.
6. G. Danby et al, Columbia University Report - June 1962.

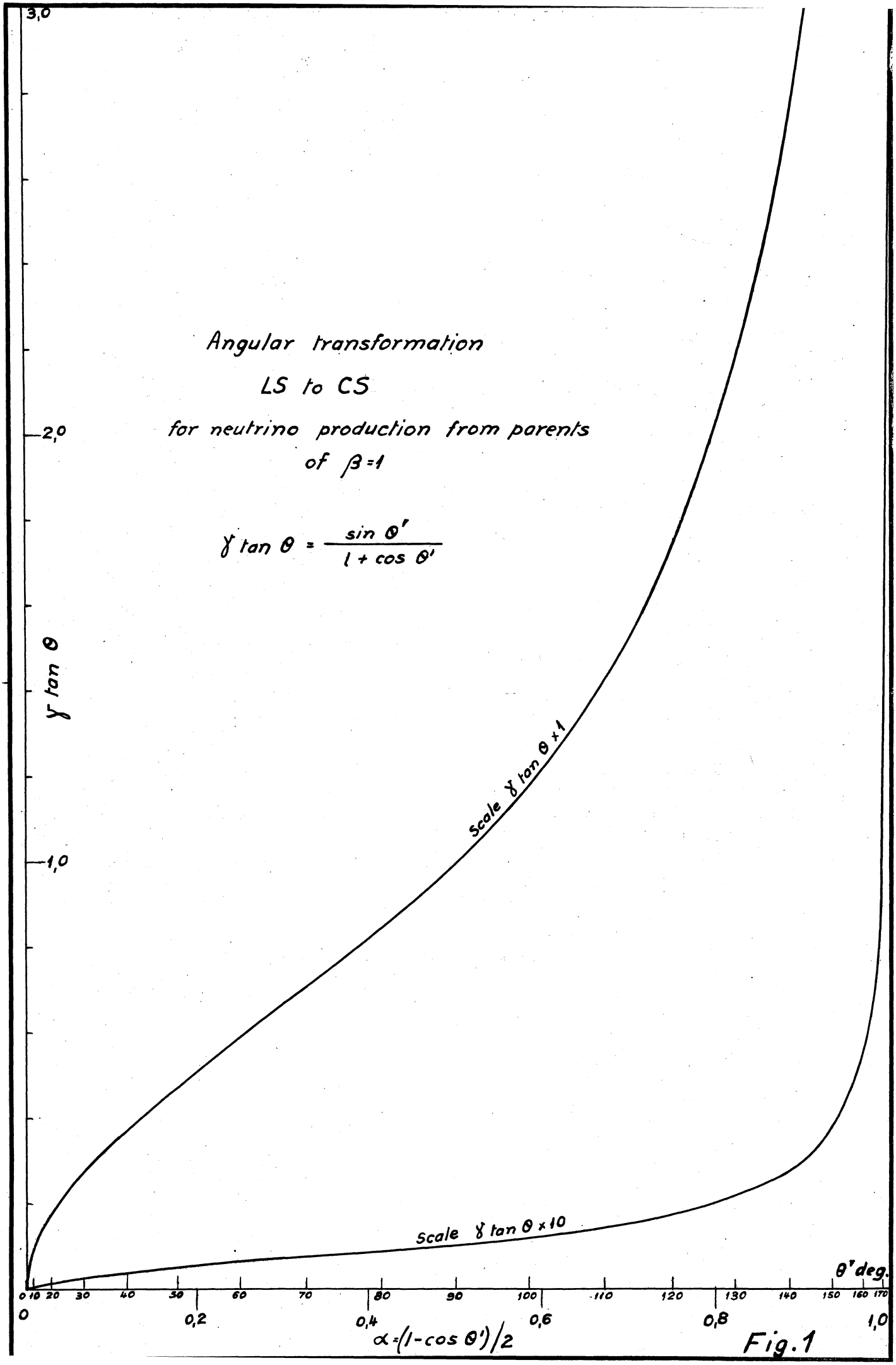
Angular transformation
LS to CS
for neutrino production from parents
of β=1
$\gamma \tan\theta = \frac{\sin\theta'}{1+\cos\theta'}$
3,0
2,0
1,0
γ tan θ
Scale γ tan θ x 1
Scale γ tan θ x 10
θ' deg.
0 10 20 30 40 50 60 70 80 90 100 110 120 130 140 150 160 170
0
0,2
0,4
0,6
0,8
1,0
α=(1-cos θ')/2

Fig. 1

ENERGY DISTRIBUTION

IN TWO BODY DECAY

WITH NEUTRINO

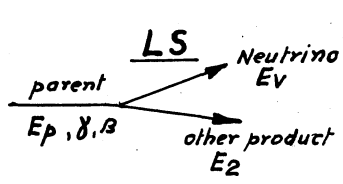

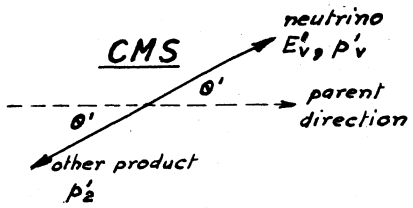

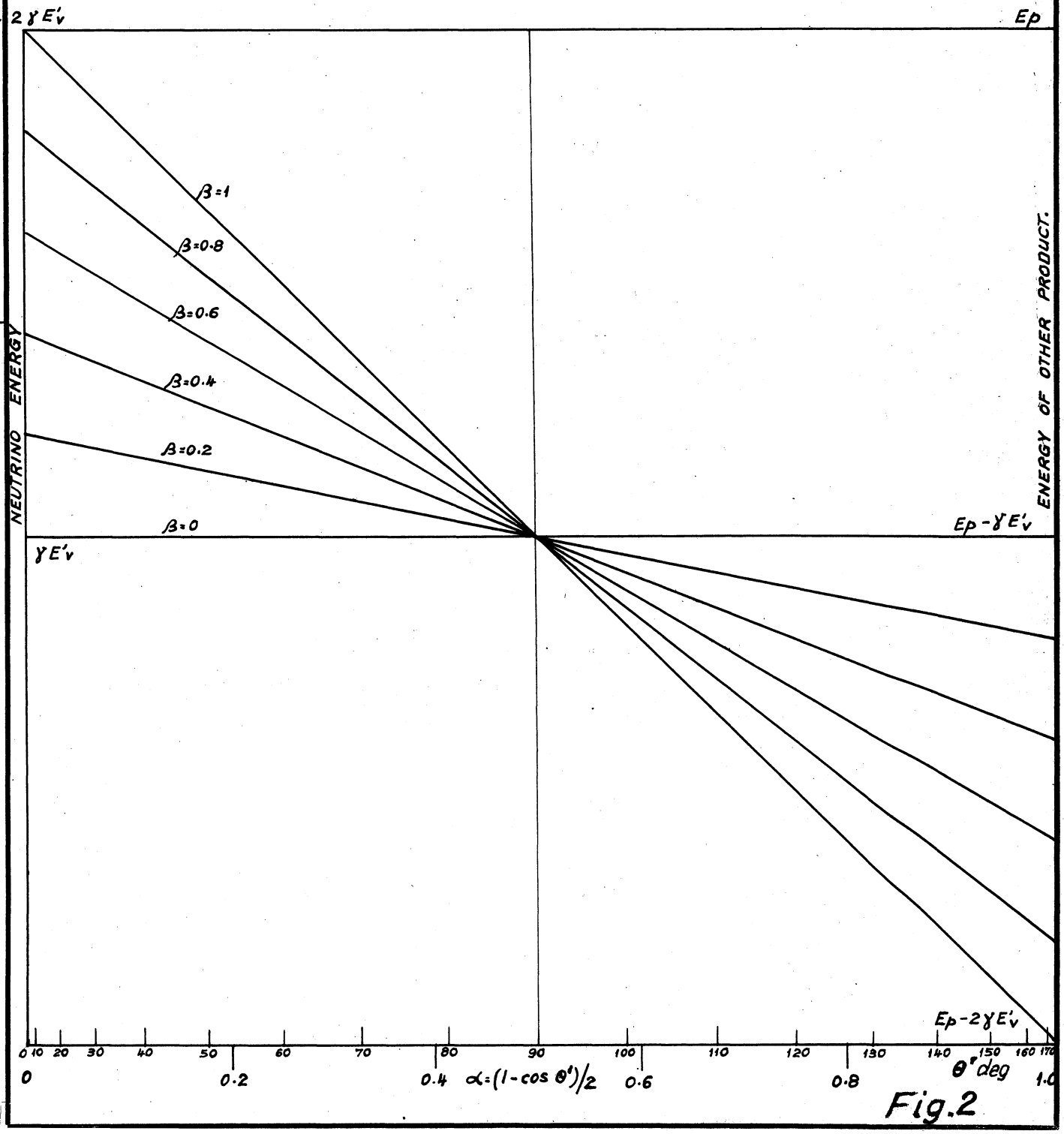

Fig.2

S/R/7469

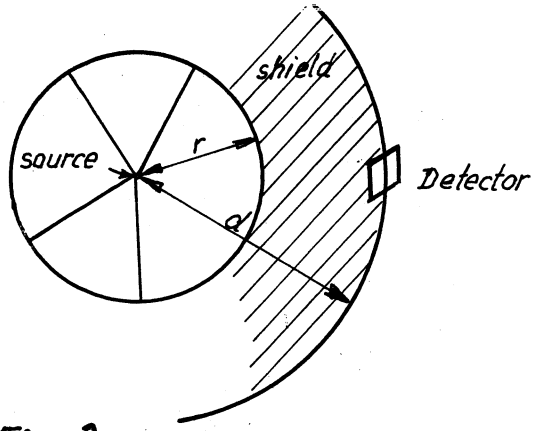

Fig. 3

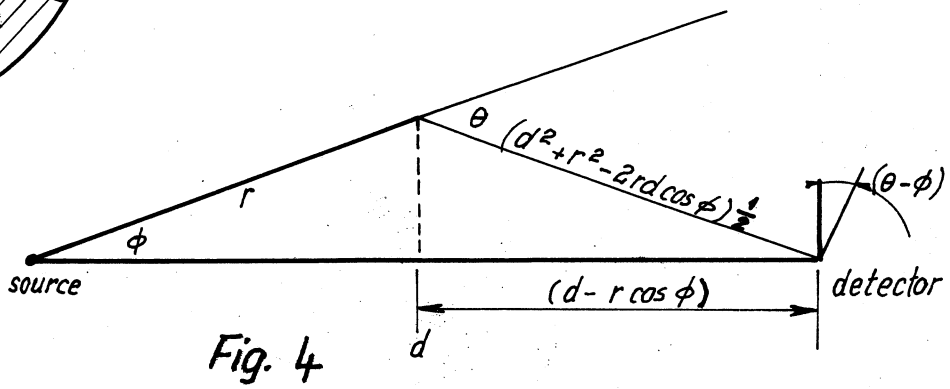

Fig. 4

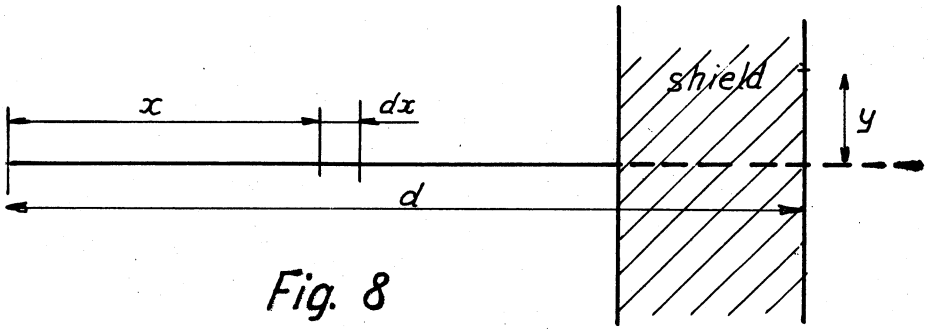

Fig. 8

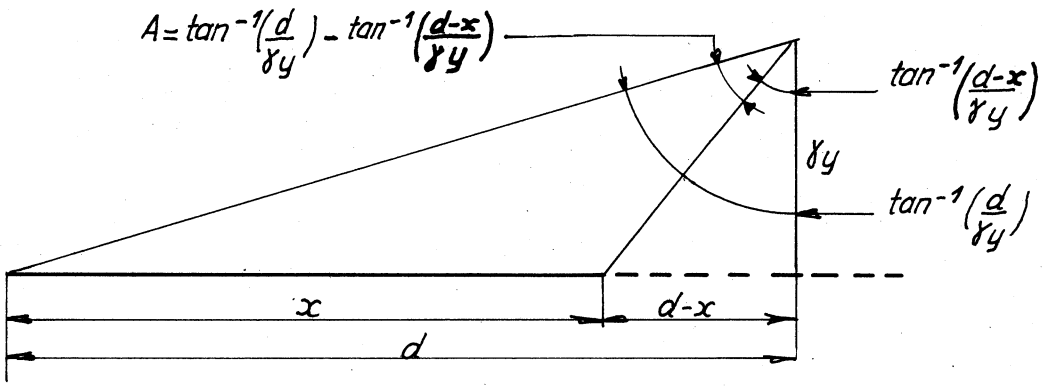

Fig. 9

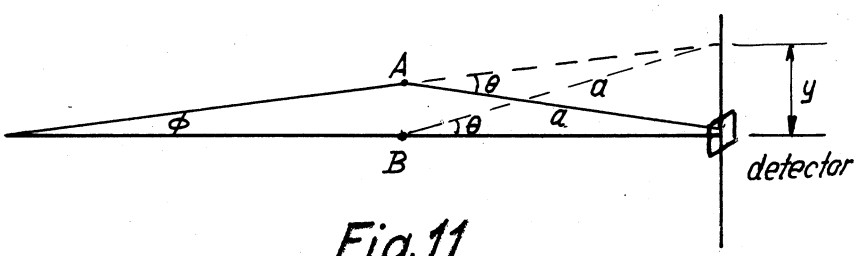

Fig. 11

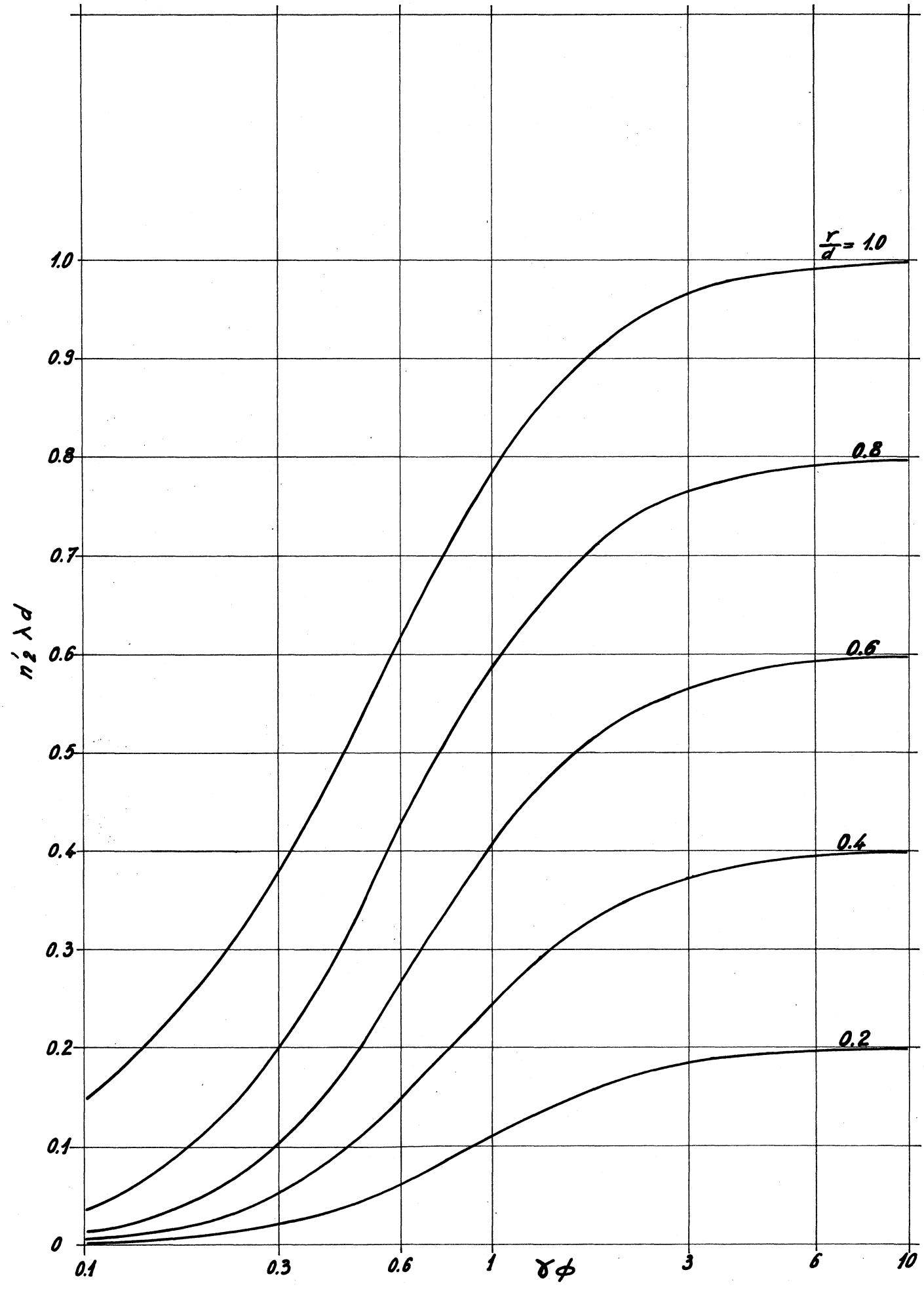
$\frac{r}{d} = 1.0$
0.8
0.6
0.4
0.2
$n'_2 \lambda d$
1.0
0.9
0.8
0.7
0.6
0.5
0.4
0.3
0.2
0.1
0
0.1
0.3
0.6
1
$\gamma\phi$
3
6
10

Fig. 5

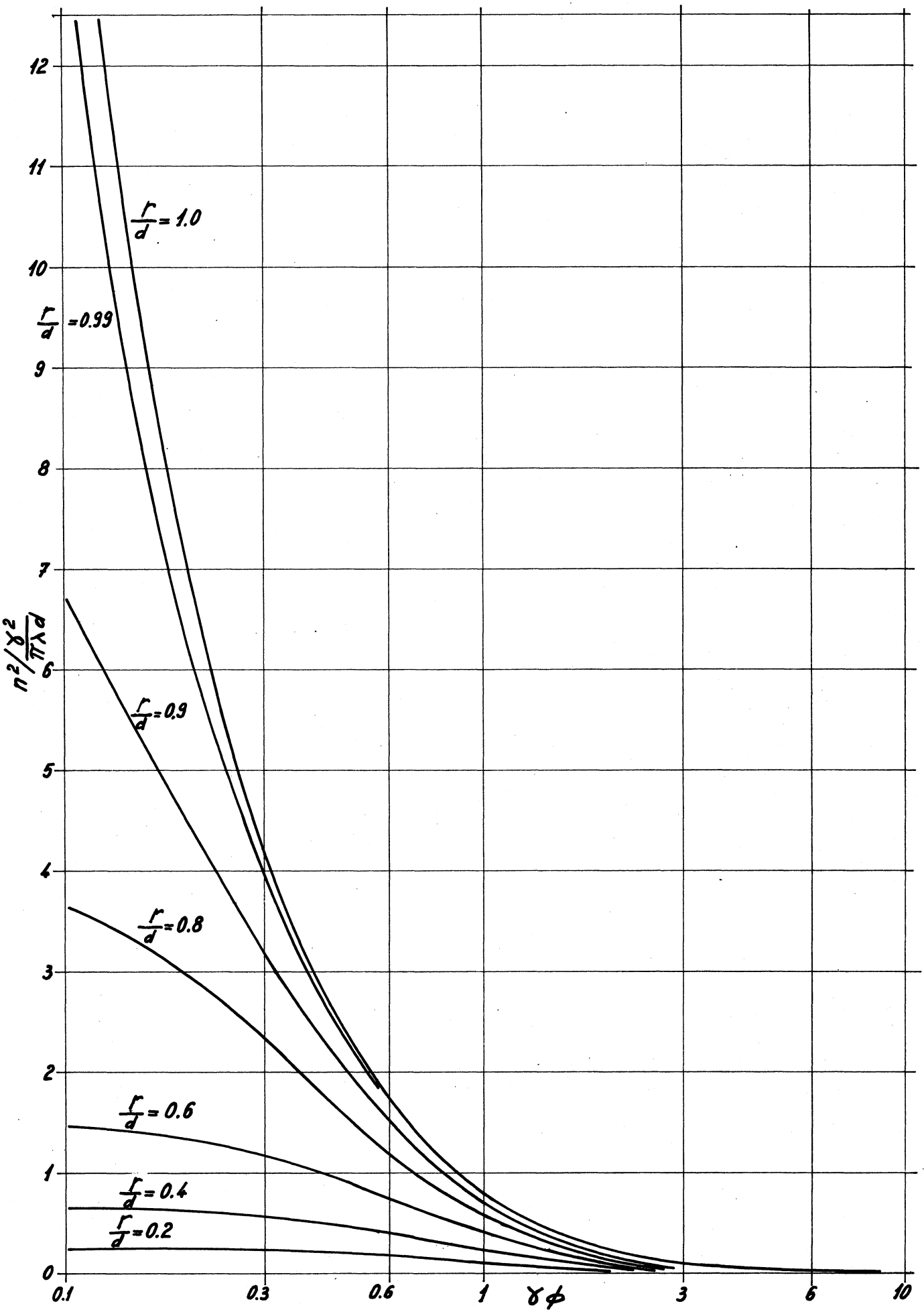
12
11
10
9
8
7
6
5
4
3
2
1
0
$\frac{r}{d}$ = 1.0
$\frac{r}{d}$ = 0.99
$\frac{r}{d}$ = 0.9
$\frac{r}{d}$ = 0.8
$\frac{r}{d}$ = 0.6
$\frac{r}{d}$ = 0.4
$\frac{r}{d}$ = 0.2
$n^2/\frac{\gamma^2}{\pi\lambda d}$
0.1
0.3
0.6
1
$\gamma\phi$
3
6
10

Fig. 6

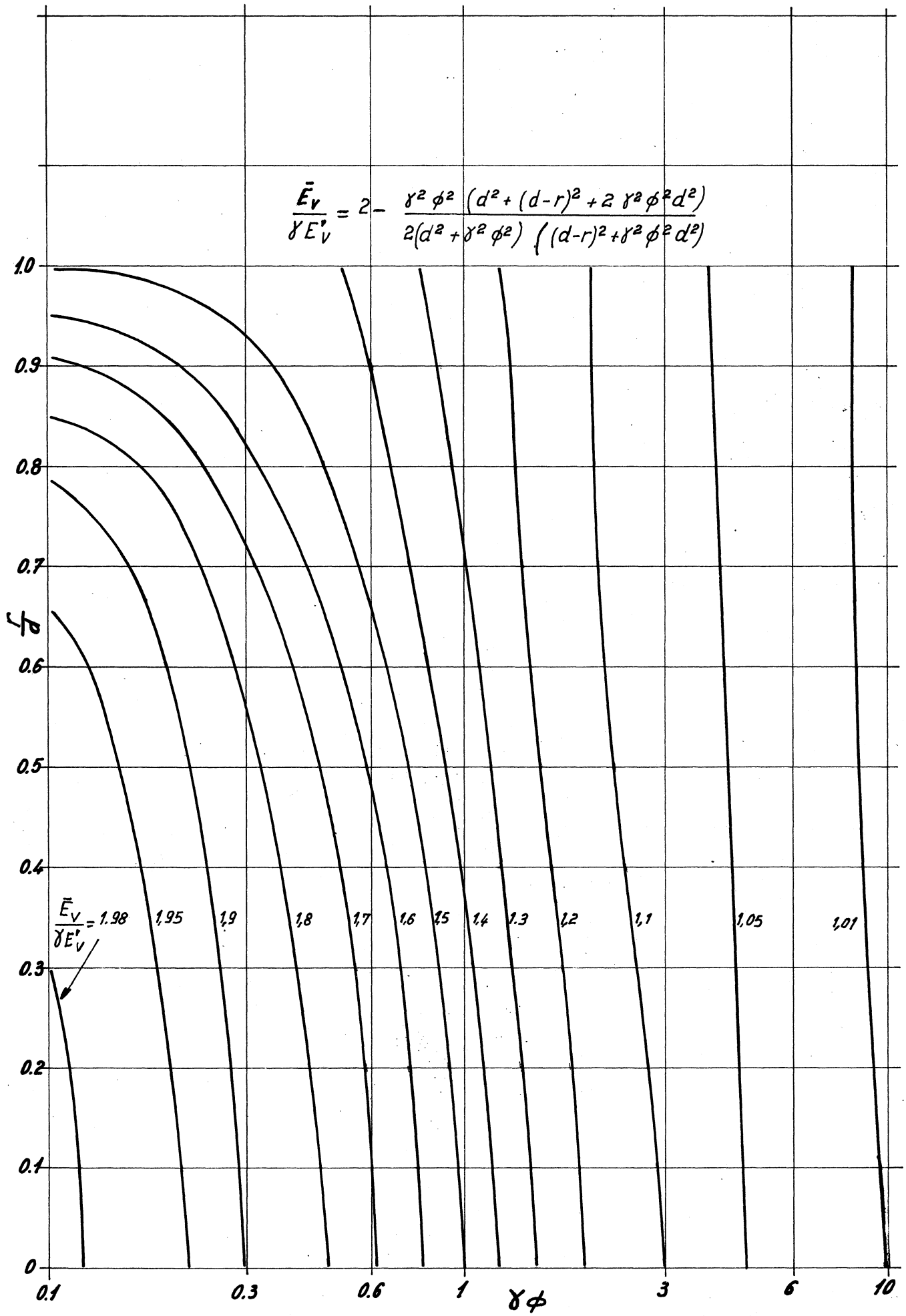

IS/R/7474 Fig. 7

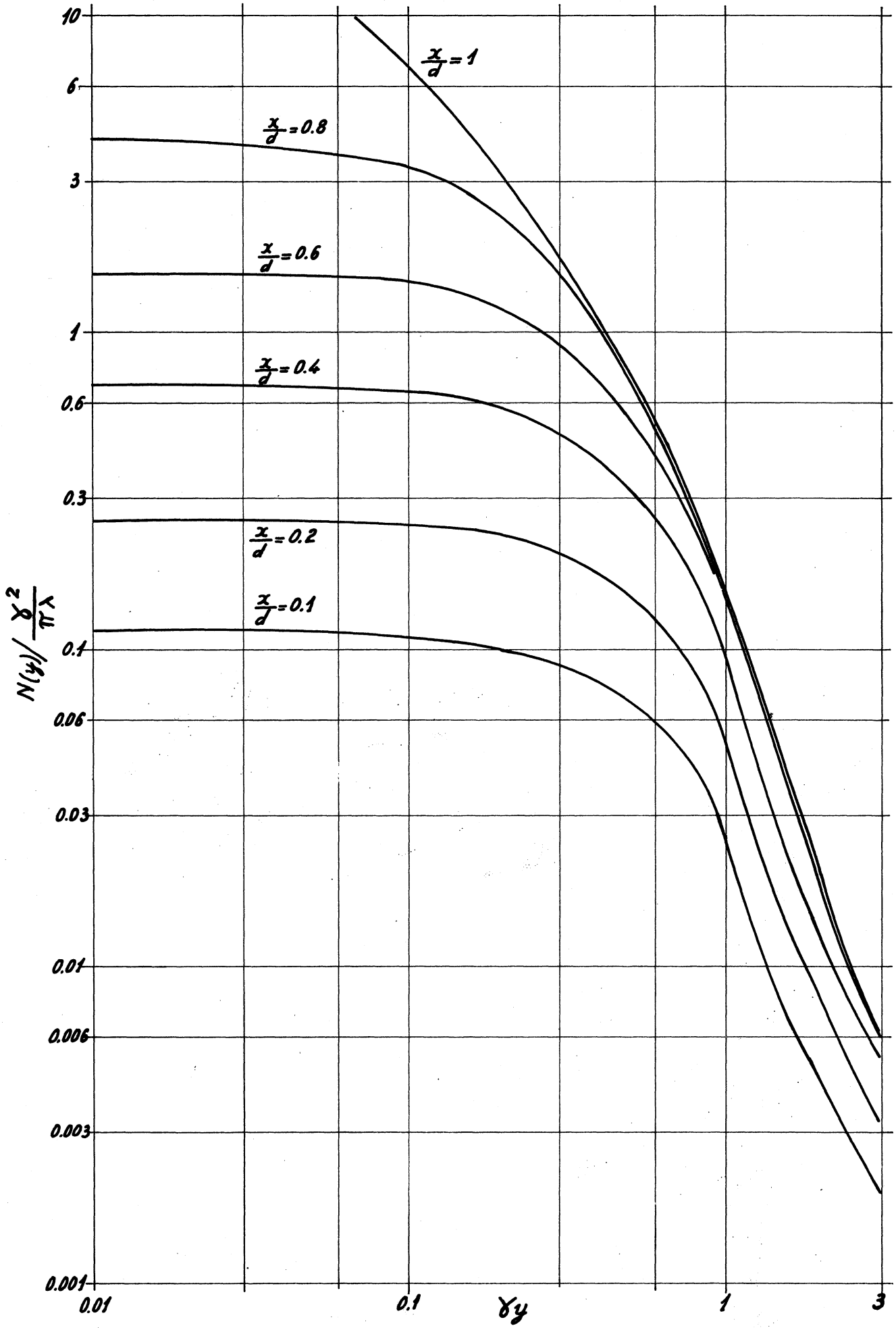

Fig. 10

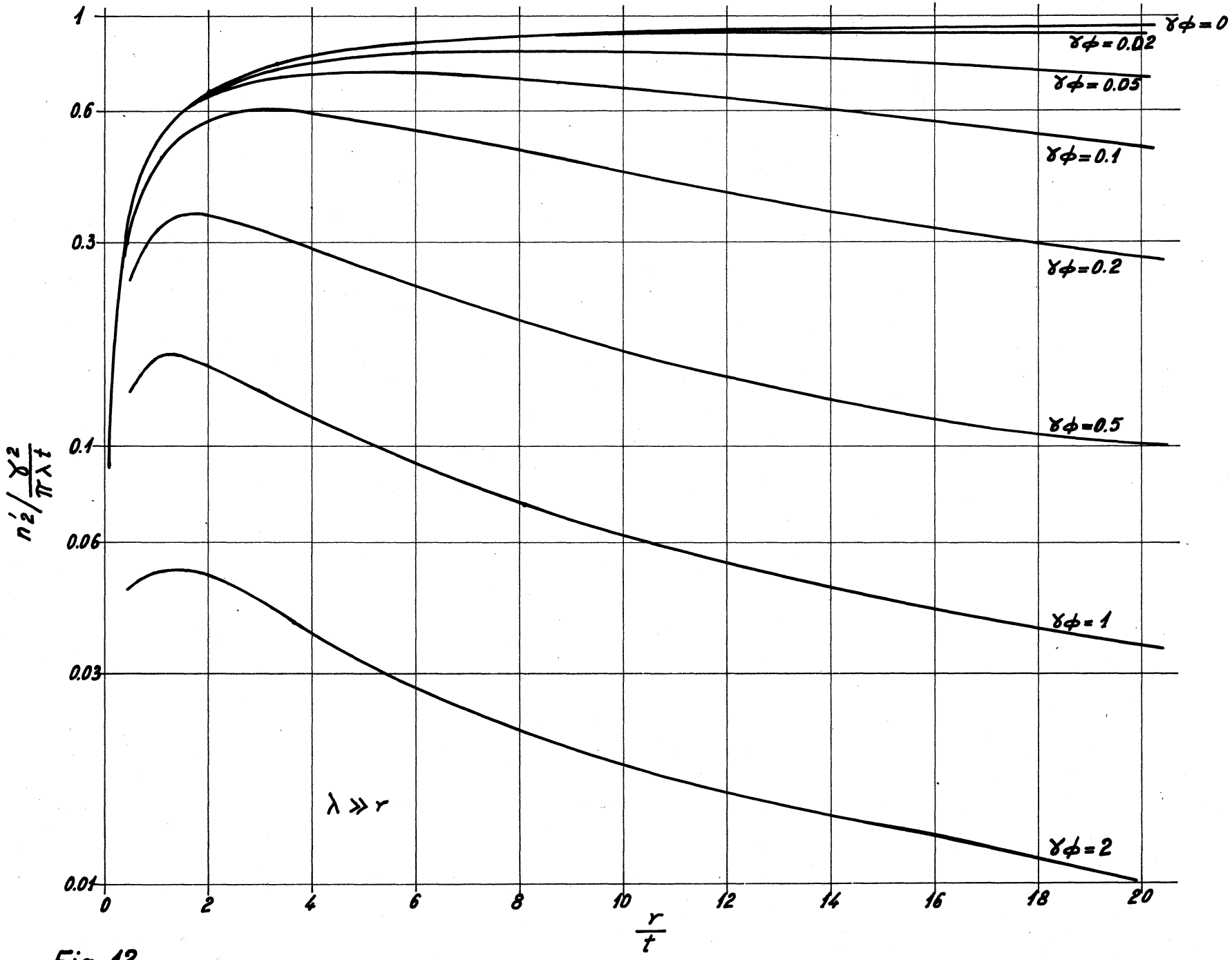

Fig. 12

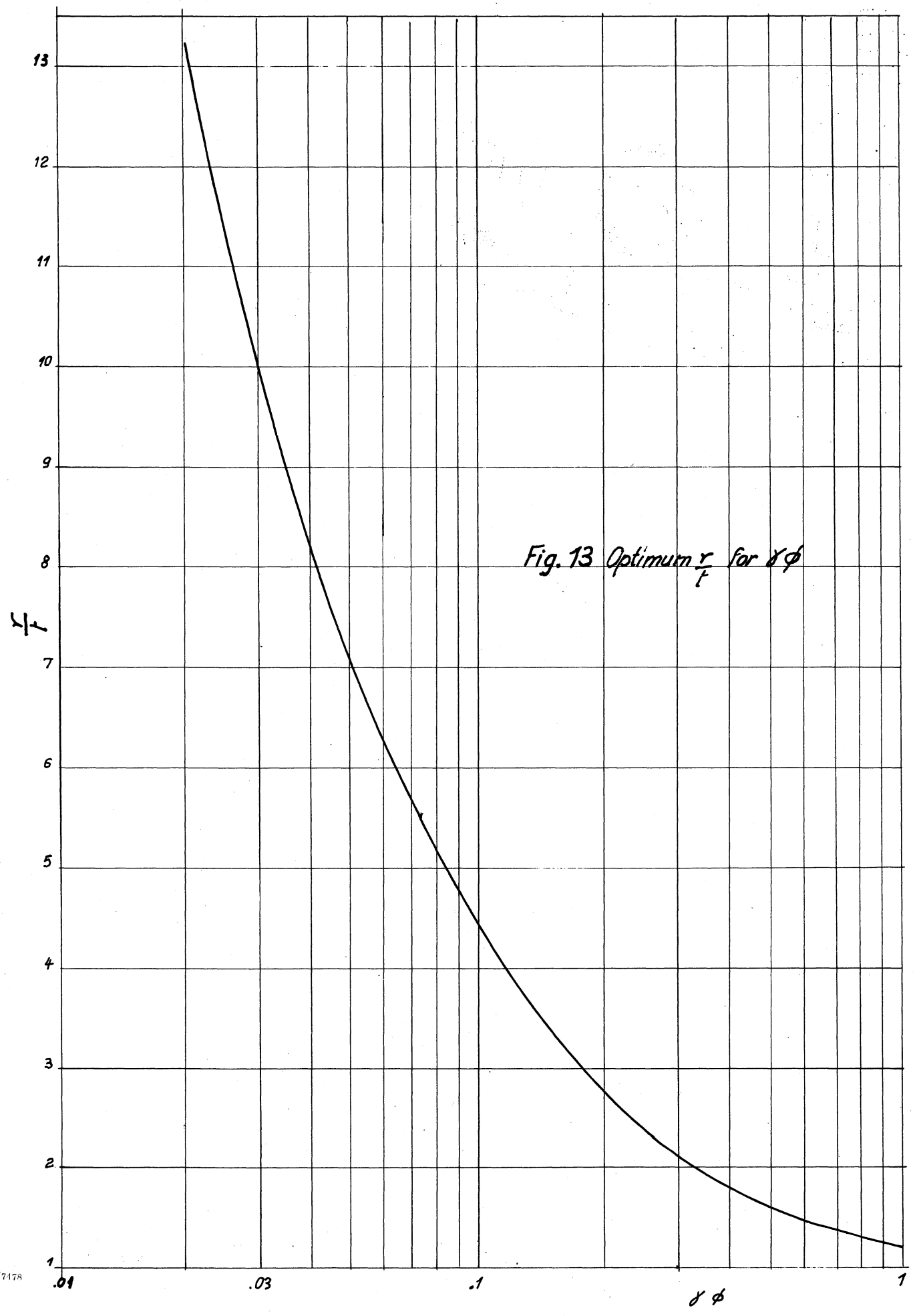

Fig. 13 Optimum $\frac{r}{t}$ for $\gamma\phi$

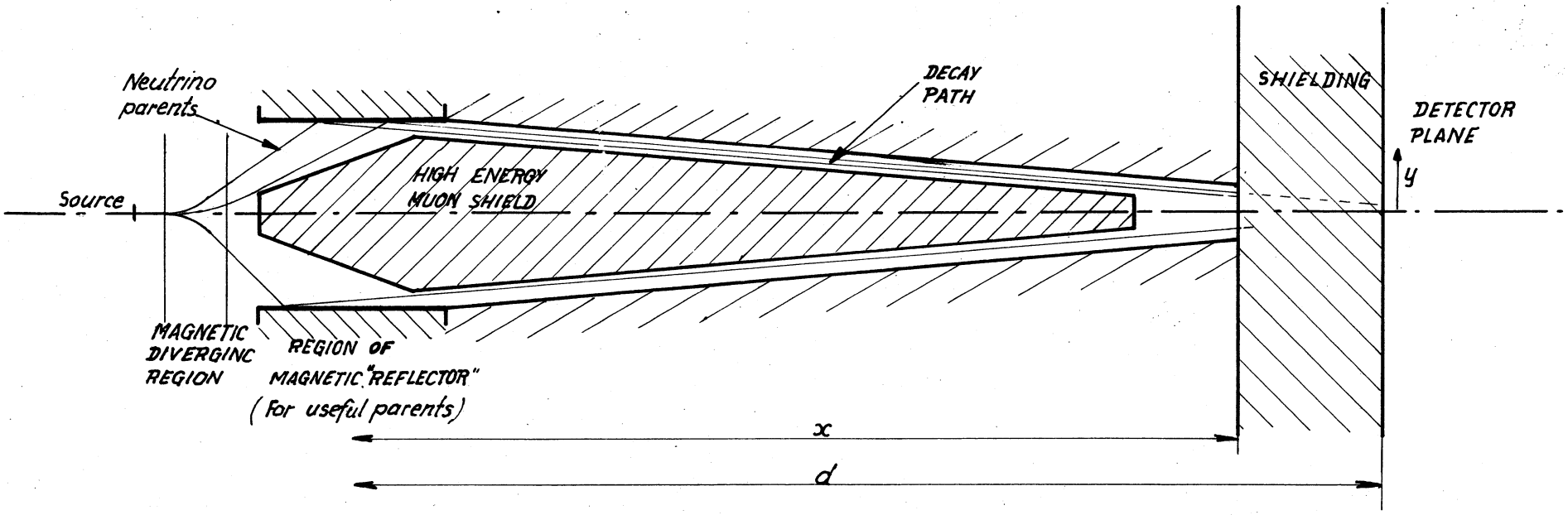

Principle of Neutrino Production from Parent Pencil

(NOT TO SCALE)

Fig. 14

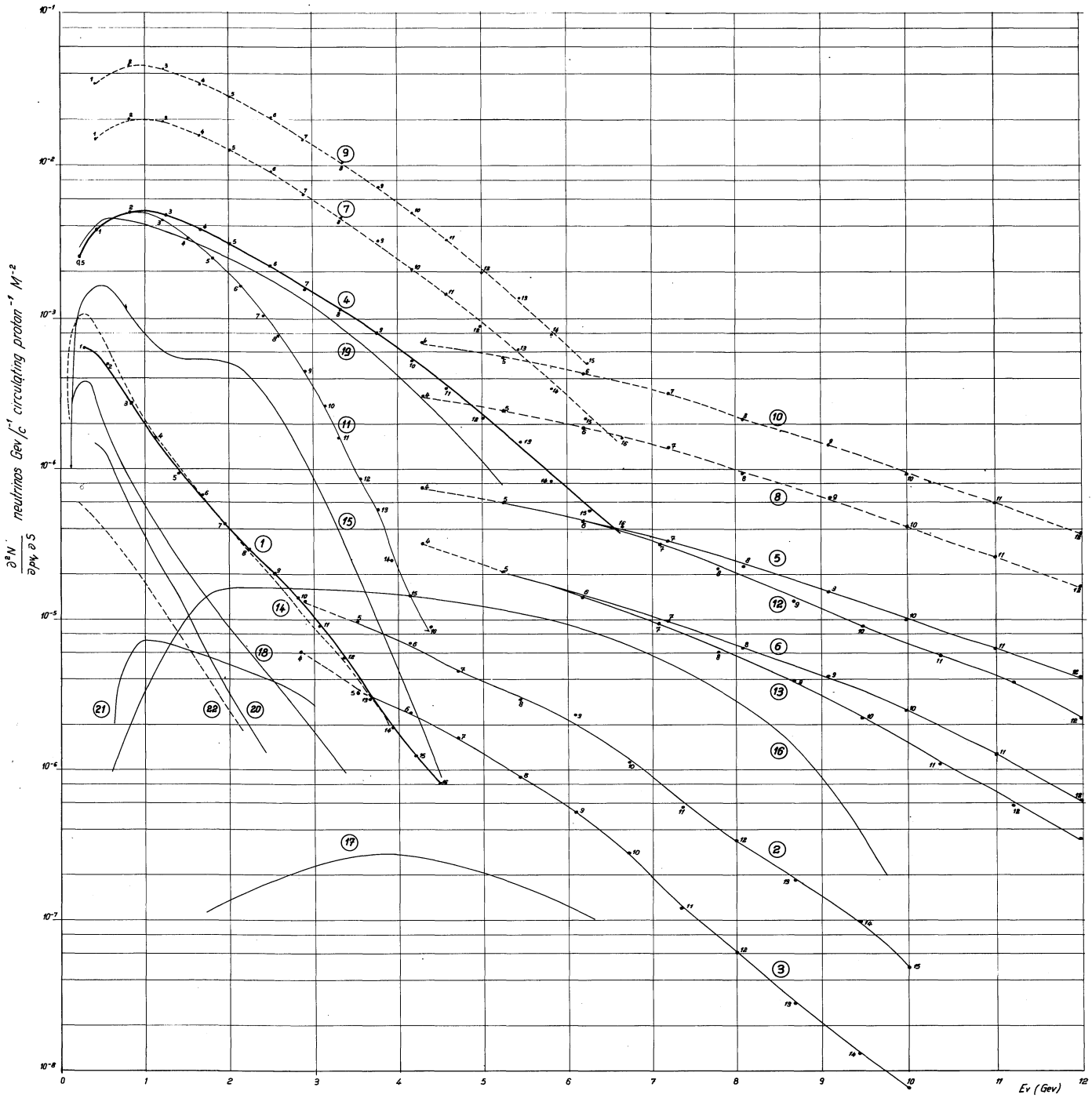
$\frac{\partial^2 N}{\partial p_\nu \partial \Omega}$ neutrinos Gev/c^{-1} circulating proton^{-1} M^{-2}
Eν (Gev)

Fig. 15

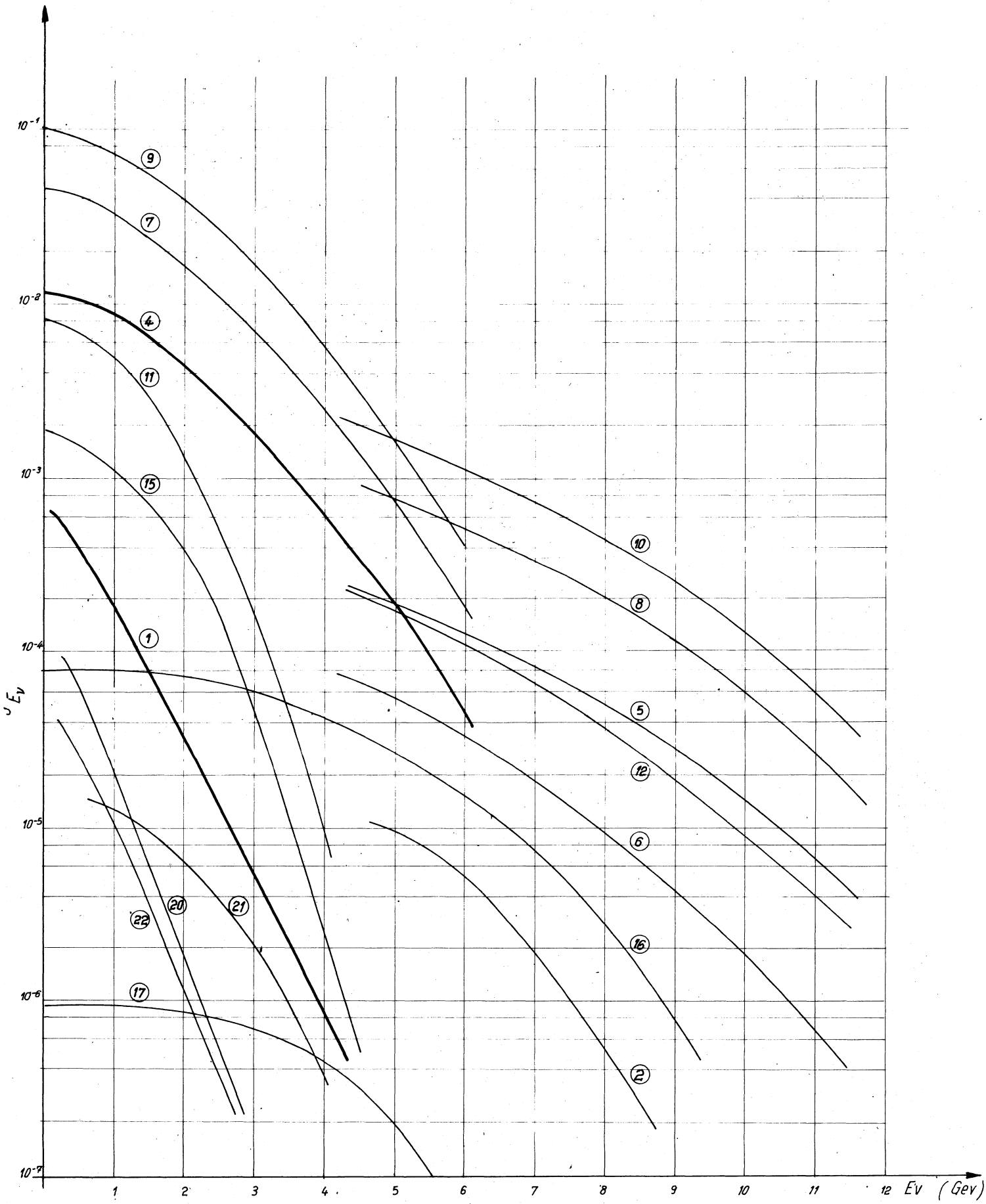
10^{-1}
10^{-2}
10^{-3}
10^{-4}
10^{-5}
10^{-6}
10^{-7}
$J E_\nu$
1
2
3
4
5
6
7
8
9
10
11
12
Ev (Gev)
9
7
4
11
15
1
10
8
5
12
6
16
2
22
20
21
17

Fig 16